Physics Letters A 376 (2012) 2781–2787

Contents lists available at SciVerse ScienceDirect

Physics Letters A

www.elsevier.com/locate/pla

Cellular automaton model in the fundamental diagram approach reproducing the synchronized outflow of wide moving jams

Jun-fang Tian *, Zhen-zhou Yuan, Bin Jia, Hong-qiang Fan, Tao Wang

MOE Key Laboratory for Urban Transportation Complex Systems Theory and Technology, Beijing Jiaotong University, Beijing 100044, People's Republic of China

ARTICLE INFO

Article history:
Received 6 April 2012
Received in revised form 2 July 2012
Accepted 21 August 2012
Available online 25 August 2012
Communicated by A.R. Bishop

Keywords:
Cellular automaton
Velocity effect
Fundamental diagram
Three-phase theory
Synchronized outflow

ABSTRACT

Velocity effect and critical velocity are incorporated into the average space gap cellular automaton model [J.F. Tian, et al., Phys. A 391 (2012) 3129], which was able to reproduce many spatiotemporal dynamics reported by the three-phase theory except the synchronized outflow of wide moving jams. The physics of traffic breakdown has been explained. Various congested patterns induced by the on-ramp are reproduced. It is shown that the occurrence of synchronized outflow, free outflow of wide moving jams is closely related with drivers time delay in acceleration at the downstream jam front and the critical velocity, respectively.

© 2012 Elsevier B.V. All rights reserved.

1. Introduction

The systematic and thorough investigation of traffic flow has quite a long history [1–10]. Various traffic phenomena have been observed, e.g. phantom jams, hysteresis effects, metastable states and stop-and-go traffic etc. Different explanations of these empirical findings and traffic flow models have been proposed. Most of these models [11–20] can be classified into the fundamental diagram approach, which postulates that the steady traffic flow belongs to a curve in the flow-density plane. However, Kerner pointed out that these models within the fundamental diagram approach cannot explain traffic breakdown and many significant features of congested patterns induced by bottlenecks (see [9,10]). Traffic breakdown simulated by these models is the transition from free flow to wide moving jams. A wide moving jam is a moving jam that maintains the mean velocity of the downstream jam front, even when the jam propagates through other traffic phases or bottlenecks. While empirical findings show that traffic breakdown is the first order transition from free flow to synchronized flow ($F \rightarrow S$ transition). In contrast with the wide moving jam phase, the downstream front of the synchronized flow phase does not exhibit the wide moving jam characteristic feature. In particular, the downstream front of the synchronized flow phase is often fixed at a bottleneck.

Based on the three phases, i.e. free flow, synchronized flow and wide moving jams, an alternative traffic flow theory called three-phase traffic theory is introduced by Kerner et al. [9,10,21–25], which can predict and explain the empirical spatiotemporal features of traffic breakdown and the resulting traffic congestion at an isolated bottleneck successfully. Empirical observations reported by Kerner [9,10] show that there are two types of congested patterns at an isolated bottleneck:

The General Patterns (GPs): After the synchronized flow occurs upstream of the bottleneck, the wide moving jams continuously emerge in that synchronized flow and propagate upstream, and then this congested pattern is often called as the General Pattern (GP). However, if the wide moving jams discontinuous emerge on the road, there will just be one or few wide moving jams appearing in that synchronized flow, then this congested pattern is often called as the dissolving general pattern (DGP).

The Synchronized Patterns (SPs): If there only exists synchronized flow upstream of the bottleneck, no wide moving jams emerge in the synchronized flow, and then this congested pattern is often called as the Synchronized Patterns. And as a result of the $F \rightarrow S$ transition, various synchronized flow patterns can occur at the bottleneck, such as the widening synchronized pattern (WSP), local synchronized pattern (LSP), moving synchronized pattern (MSP).

The fundamental hypothesis of three-phase theory is that the hypothetical steady states of the synchronized flow cover a two-dimensional region in the flow-density plane, i.e. there is no fundamental diagram of traffic flow in this theory. Subsequently, many

* Corresponding author.
E-mail address: tianhustbjtu@hotmail.com (J.-f. Tian).

0375-9601/$ – see front matter © 2012 Elsevier B.V. All rights reserved.
http://dx.doi.org/10.1016/j.physleta.2012.08.035

traffic flow models have been proposed in the framework of three-phase traffic theory [25–35]. In order to emphasize the significance of the two-dimensional steady states of synchronized flow, Kerner and Klenov proposed the speed adaption three-phase traffic models (SA models) [27] in the framework of fundamental diagram approach. The basic hypothesis of SA models is the double Z-characteristic for the sequence of phase transitions from free flow to synchronized flow to wide moving jams ($F \to S \to J$ transitions). Based on this hypothesis, SA models can reproduce both the traffic breakdown and the emergence of wide moving jams in synchronized flow as found in empirical observations. However, SA models are not able to reproduce the local synchronized patterns (LSPs) consistent with empirical results as well as some of empirical features of synchronized flow between wide moving jams within general patterns (GPs). Kerner et al. attribute these drawbacks of SA models to the lacking of the two-dimensional steady states of synchronized flow. At the same time, it is worth saying that models in the three-phase theory, such as the KKW model [28], could not reproduce some empirical findings as well. The KKW model cannot simulate a single moving synchronized pattern (MSP) as well as an LSP whose width changes over time observed in real traffic [29].

Recently, a simple cellular automaton named the average space gap model (ASGM) [36] within the fundamental diagram approach was proposed to reproduce some empirical findings of the three-phase traffic theory. ASGM can reproduce the $F \to S \to J$ transitions, the single MSP, and other congested patterns induced by an on-ramp that are in line with empirical results. However, the synchronized outflow of wide moving jams cannot be reproduced by ASGM. Thus, ASGM needs to be improved since this defect leads to the absence of only synchronized flow existing between wide moving jams in GP, which is one of the key aspects of the criticisms that three-phase theory is made on the fundamental diagram approach. In this Letter, an improved ASGM is established by taking the velocity effect and critical velocity into account. The physics of traffic breakdown and the mechanism of the synchronized outflow and free outflow of wide moving jams are explained by the improved model.

2. The model

The essential mechanisms to reproduce three-phase traffic theory in the improved model are embodied in the randomization process of vehicles. The parallel update rules are as follows.

(1) Definition of the average safe space gap $d_n^{avg}(t)$

$$d_n^{avg}(t) = \left\lfloor \sum_{i=n}^{m_l+n} d_i^{eff}(t)/(m_l+1) \right\rfloor$$

(2) Determination of the randomization parameter $p_n(t+1)$ and deceleration extent Δv:

$$p_n(t+1) = \begin{cases} p_a: & \text{if } v_n(t) > \max(d_n^{avg}(t), v_c) \\ p_b: & \text{if } v_n(t) = 0 \text{ and } t_n^{st}(t) \geqslant t_c \\ p_c: & \text{otherwise} \end{cases} \quad (1)$$

$$\Delta v(t+1) = \begin{cases} a: & \text{if } v_n(t) > \max(d_n^{avg}(t), v_c) \\ b: & \text{otherwise} \end{cases} \quad (2)$$

(3) Acceleration:

$$v_n(t+1) = \min\bigl(v_n(t)+1, v_{max}\bigr)$$

(4) Deceleration:

$$v_n(t+1) = \min\bigl(d_n^{eff}(t), v_n(t+1)\bigr)$$

(5) Randomization with probability $p_n(t+1)$:

$$\text{if } \bigl(rand() < p_n(t+1)\bigr)$$
$$\text{then } v_n(t+1) = \max\bigl(v_n(t+1) - \Delta v(t+1), 0\bigr)$$

(6) Car motion:

$$x_n(t+1) = x_n(t) + v_n(t+1)$$

$\lfloor x \rfloor$ denotes the maximum integer that is not bigger than x. $d_n^{eff}(t) = d_n(t) + \max(0, \min(v_{n+1}(t)+1, d_{n+1}(t), v_{max}) - d_{safe})$ is the safe space gap between vehicle n and its preceding vehicle $n+1$, and d_{safe} is the safe factor to avoid accidents. $d_n(t)$ is the actual gap, $d_n(t) = x_{n+1}(t) - x_n(t) - L_{car}$. $x_n(t)$ is the position of vehicle n (here vehicle $n+1$ precedes vehicle n). This is the velocity effect that the velocity of vehicle n depends not only on the positions of itself and vehicle $n+1$, but also on the velocity of vehicle $n+1$. L_{car} is the length of the vehicle, and $v_n(t)$ is the velocity of the vehicle n. $t_n^{st}(t)$ denotes the time that a car stops. When the car has stopped for a certain time that is larger than or equal to t_c, the driver will become less sensitive. $d_n^{avg}(t)$ is defined to model the anticipation effect of taking m_l vehicles in front into account. In order to describe it, the value of m_l should be large enough, suggesting $m_l \geqslant 2$. v_c is the critical velocity to simulate the situation that when the speed is smaller enough, the driver will not take $m_l - 1$ vehicles in front of the leading vehicle into account. If d_{safe} and v_c are set as $\min(v_{n+1}(t)+1, d_{n+1}(t), v_{max})$ and zero respectively, ASGM can be obtained. This improved model is named the improved averaged space gap cellular automaton model, abbreviated as IASGM.

The basic driver behaviors in IASGM are as follows: (i) for sufficiently large space gaps in free flow, drivers will accelerate until the maximum speed v_{max}, since d_n^{avg} and d_n^{eff} is greater than or equal to v_{max}. Behaviors of this kind can be named as free driving effect, which is realized by rule (3) in IASGM. (ii) For relatively small space gaps in synchronized flow, drivers have to trade between d_n^{avg} and d_n^{eff}. If d_n^{avg} is higher than d_n^{eff}, the driver will adjust to d_n^{eff}; otherwise, the driver will turn up to d_n^{avg}. Furthermore, drivers become more defensive when the actual speed is higher than d_n^{avg}. The actual behavioral change is characterized by increasing the randomization probability from p_c to p_a, and the associated deceleration from b to a. This behavior is named as anticipation driving effect, which is fulfilled by rules (4) and (5) in IASGM.

3. Fundamental diagram

Fundamental diagram approach postulates that the steady traffic flow forms a curve in the flow-density plane. Correspondingly, this curve going through the origin with at least one maximum is called the fundamental diagram for traffic flow. In the unperturbed, noiseless limit, models within the fundamental diagram approach will have a fundamental diagram of steady states [10]. The fundamental diagram is either hypothesized in these models (e.g. the optimal velocity model [18]), or the fundamental diagram is a result of these models (e.g. the Nagel–Schreckenberg cellular automaton model (NaSch model) [17]).

In what follows, we show that the steady states of IASGM have a fundamental diagram of steady states in the unperturbed, noiseless limit according to Kerner's method [10]. Since the mechanisms associated with the synchronized flow in IASGM are all embodied in the randomization process, the noiseless limit should be taken as $p_a = 1$, $p_c = 0$, $p_b = 0$ or $p_a = 1$, $p_c = 1$, $p_b = 1$. However, all vehicles will keep stationary no matter how far distance between vehicles in the latter case, which is obviously unrealistic. Thus, we just consider the former. Steady states of traffic flow

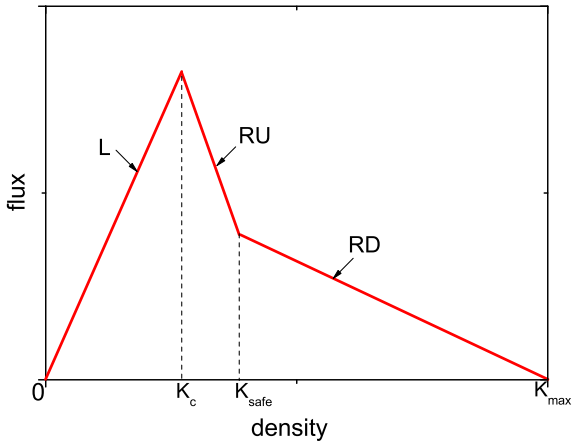

Fig. 1. Fundamental diagram of IASGM. The lines L, RU, and RD are determined by $J = Kv_{max}$, $J = 2 - KL_{car} - \frac{K}{K_{safe}}$ and $J = 1 - KL_{car}$, respectively. (See Appendix A for the derivation for the fundamental diagram and the meaning of the parameters.)

are hypothetical states of homogeneous (in time and space) traffic flow of identical vehicles (and identical drivers) in which all vehicles move with the same time-independent speed and have the same space gaps [10]. Therefore, d_n^{avg} should equal to d_n^{eff}. According to model rule (4), v_n will always be no more than d_n^{eff}. Thus, $v_n \leqslant d_n^{avg}$ and $p_n = p_c$. On the basis of rules (2), (3) and (4), the steady states are given by the equality: $v_n = d_n^{eff}$. This condition together with $v_n \leqslant v_{max}$ defined the steady state of the IASGM: $v_n = \min(d_n^{eff}, v_{max})$. This equation can be written as the conditions for the gap d and the vehicle speed v: $v = \min(d + \max(0, \min(v+1, d, v_{max}) - d_{safe}), v_{max})$, which form a curve of the steady states in the flow-density plane, i.e. the fundamental diagram (see Fig. 1, see Appendix A for the derivation for the fundamental diagram).

4. Simulations and discussions

Simulations are implemented on a road with length $L_{road} = 5000L_{cell}$. Each cell has the length of $L_{cell} = 1.5$ m, and the length of a vehicle is $L_{car} = 7.5$ m, i.e. five cells could accommodate only one vehicle ($L_{car} = 5$). The maximum velocity v_{max} is set as $v_{max} = 20$, and the velocity of each vehicle is an integer, which ranges from 0 to v_{max}. One time step corresponds to 1 s. The other parameters are as follows: $p_a = 0.95$, $p_b = 0.5$, $p_c = 0.03$, $a = 3$, $b = 1$, $t_c = 4$, $m_l = 3$, $d_{safe} = 7$, $v_c = 3$. During the simulations, first 10 000 time steps are discarded to let the transient time die out.

Simulations are carried out near an on-ramp under open boundary condition. The vehicles move from left to right. The left-most cell corresponds to $x = 1$. The position of the left-most vehicle is x_{last} and that of the right-most vehicle is x_{lead}. At each time step, if $x_{last} > v_{max}$, a new vehicle with velocity v_{max} will be injected to the position $\min(x_{last} - v_{max}, v_{max})$ with probability q_{in}. If $x_{lead} > L_{road}$, the leading vehicle will be removed and the following vehicle becomes the leader.

A simple method is adopted to model the on-ramp [34]. Assuming the position of the on-ramp is x_{on}, a region $[x_{on}, x_{on} + L_{on\text{-}ramp}]$ is selected as the inserting area of the vehicle from on-ramp. At each time step, the longest gap in this region is found out. If the gap is large enough for a vehicle, then a new vehicle will be inserted at the cell in the middle of the gap with probability q_{on}. The velocity of the inserted vehicle is set as the velocity of its preceding vehicle, and the stop time is set to zero. The parameters are set as $x_{on} = 0.8L_{road}$ and $L_{on\text{-}ramp} = 50$.

4.1. The physics of traffic breakdown

According to the basic driver behaviors in IASGM, a competition between two opposite tendencies can be found, i.e., the tendency towards to free flow due to the free driving effect and the tendency towards to synchronized flow owing to the anticipation driving effect. This competition occurs within a local disturbance in which the speed is lower and density is higher than in the initial free flow.

Due to this competition, traffic breakdown phenomenon can be explained as follows: free flow maintains on the road provided that the free driving effect is stronger than the anticipation driving effect when the density is small enough on the road, i.e., the space gaps between vehicles are large enough. However, the greater the density the smaller the space gaps, the weaker the free driving effect and the stronger the synchronized driving effect. After the critical point is exceeded, where the free driving effect works the same as the synchronized driving effect, traffic breakdown happens and synchronized flow begins to emerge in free flow.

This competition is shown in Fig. 2, which exhibits the spatiotemporal characteristic of MSP. At the time interval between 21 800 s and 21 850 s, vehicles 1, 2 are inserted in the on-ramp region. The inserted vehicle 1 leads to the first disturbance. Due to the small space gaps from vehicle 3 to vehicle 12, each following vehicle moving in front of vehicle 11 must slow down when entering into the disturbance, which means the predominance of the anticipation driving effect. However, since the large distance between vehicle 5 and vehicle 6, vehicle 7 and vehicle 8, vehicle 9 and vehicle 10, the anticipation effect become more and more weaker, the free driving effect is getting stronger when this disturbance propagates upstream. Due to the large distance between vehicle 11 and vehicle 12, the anticipation effect is weaker than the free driving effect. As a result, the speed of vehicle 12 just slightly fluctuates and reverts to the free speed quickly, i.e. the first disturbance diminishes. The inserted vehicle 2 causes another disturbance, and the speed of the following vehicles decrease. Owing to the small space gaps between them, the anticipation driving effect is stronger than the free driving effect. Consequently, the speed fluctuations grow and propagate upstream, leading to occurrence of MSP.

Moreover, it is known that traffic breakdown has the probabilistic nature at a bottleneck, i.e., at a given upstream flow rate of a bottleneck, traffic breakdown could occur or not [9,10,37–39]. In order to investigate this property at the on-ramp, the method proposed by Kerner et al. [28] is applied. N_p simulations of the same time interval T_0 are carried out for the given rates q_{sum} and q_{on}, where $q_{sum} = q_{in} + q_{on}$. For each simulation, whether breakdown occurs within T_0 has been checked. The result of N_p simulations is the number of realizations n_p where breakdown occurs. Then $p_{FS}^{(B)} = n_p/N_p$ is the approximate probability the traffic breakdown happens in an initial free flow during the time interval T_0. Fig. 3 shows that the probability that traffic breakdown happens within a given time interval increases exponentially with the flux q_{sum}, which is in accordance with the empirical findings and the simulations result of models in the three-phase theory.

4.2. Spatiotemporal congested patterns

When traffic breakdown happens near the on-ramp, various congested patterns can occur. These congested patterns are plotted in Fig. 4. Different values of q_{in} and q_{on} have induced six distinct congested patterns predicted by the three-phase theory. In Fig. 4(a), the spatial-temporal features of moving synchronized flow (MSP) are shown. In this pattern, synchronized traffic flow spontaneously emerges in the free flow. Both the downstream front and upstream front of MSP propagate upstream. Fig. 4(b)

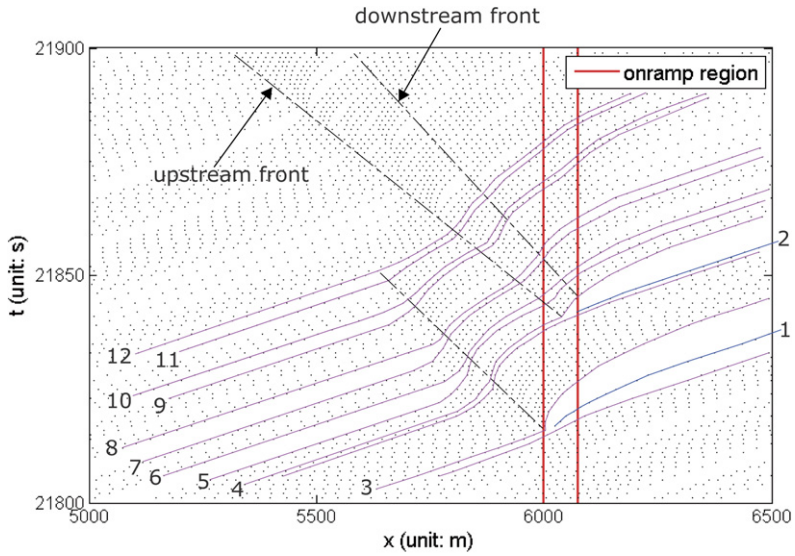

Fig. 2. Trajectories of vehicles in MSP. $(q_{in}, q_{on}) = (0.7, 0.02)$. The lines marked by upstream front and downstream front represent the upstream front and downstream front of MSP. The line marked by onramp means the region of the on-ramp on the road. The lines marked by numbers denote the trajectories of the numbered vehicles. The horizontal direction (from left to right) is space (unit: m) and the vertical direction (from down to up) is time (unit: s).

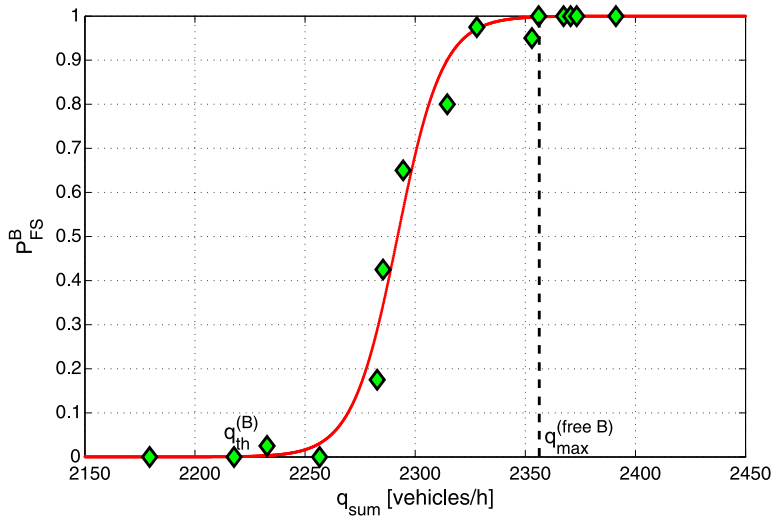

Fig. 3. Probability of breakdown phenomenon at the on-ramp within $T_0 = 60$ min, after the on-ramp flow was switched on. The result is obtained when $q_{in} = 0.6$ and q_{on} increases gradually. The criterion to determine the occurrence of breakdown is that the vehicle speed upstream of the on-ramp drops below 80 km/h for more than 2 min. The curve is fitted with the function $p_{FS}^{(B)} = (1 + \tanh(a(q_{sum} - b)))/2$, where $a = 0.04876$, $b = 2292$ and R-square equals 0.985. $q_{th}^{(B)}$ is the minimum highway capacity. When $q_{sum} \leqslant q_{th}^{(B)}$, no traffic breakdown will occur, since the probability equals zero. $q_{max}^{(free\ B)}$ is the maximum highway capacity. When $q_{sum} \geqslant q_{th}^{(B)}$, traffic breakdown occurs, since the probability equals one.

exhibits the widening synchronized flow (WSP). The downstream front of WSP is fixed at the on-ramp and the upstream front of WSP propagates upstream continuously over time. In Fig. 4(c), the downstream front of synchronized flow is also fixed at the on-ramp. However, differing with WSP, the upstream front of synchronized flow is not continuously widening but fluctuates as time going. The region of synchronized flow is limited near the on-ramp. Thus, it belongs to the local synchronized pattern (LSP). Fig. 4(d) shows the dissolving general patterns (DGP) in which just one wide moving jam emerges in the synchronized flow, which means the $S \to J$ transition could be reproduced by IASGM. Fig. 4(e) shows the spatial-temporal features of general pattern (GP). One can see that a sequence of wide moving jams occurs in synchronized flow in GP.

It is necessary to illustrate the difference among IASGM, ASGM and SA models, since IASGM is based on ASGM and all of which are in the framework of fundamental diagram approach. SA models have been criticized because they could not reproduce some empirical phenomena, i.e. LSPs and GPs consistent with empirical data. The LSPs reproduced by SA models are very narrow ones, which are localized within the merging regions of the on-ramp and consist of two narrow fronts only. And there is no synchronized flow between the fronts within these LSPs. Fig. 4(c) shows that the width of LSP reproduced by IASGM in the longitudinal direction changes over time, which is in accordance with empirical observations. Moreover, only free flow can be formed in the downstream front of wide moving jams within the GP in SA models, which is also the truth for ASGM. However, Fig. 4(f) shows that the state that only synchronized flow exists between wide moving jams in GP could be simulated if one reduce the value of the slow-to-start probability p_b. It is known to all that the slow-to-start probability p_b is close with $\tau_{del,jam}^{(a)}$, i.e., the driver time delay in acceleration at the downstream jam front. Reducing p_b is equivalent to decreasing $\tau_{del,jam}^{(a)}$, which means decreasing the average

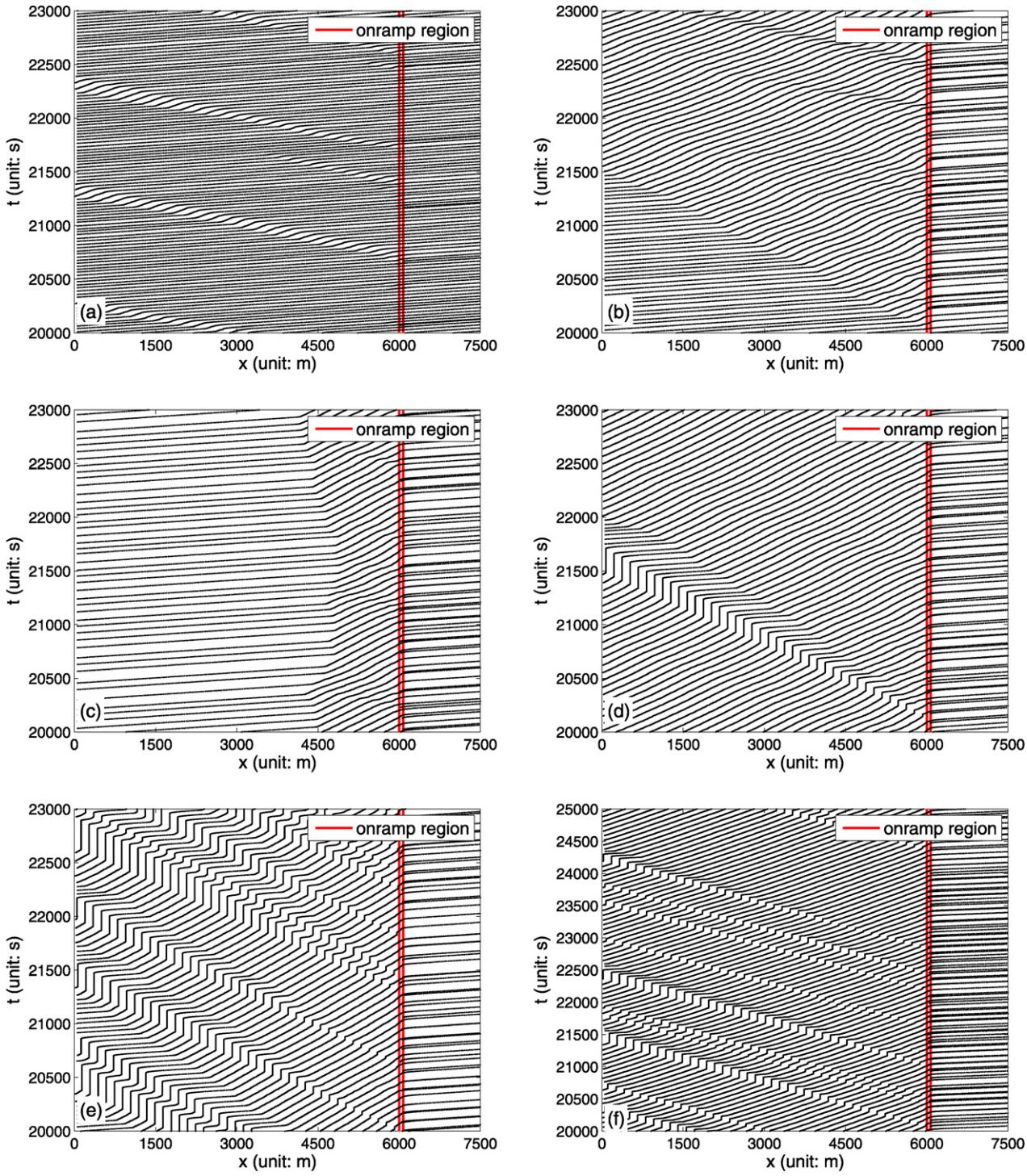

Fig. 4. Trajectories of every 20th vehicle. (a) $(q_{in}, q_{on}) = (0.7, 0.03)$ (MSP), (b) $(q_{in}, q_{on}) = (0.5, 0.2)$ (WSP), (c) $(q_{in}, q_{on}) = (0.3, 0.24)$ (LSP), (d) $(q_{in}, q_{on}) = (0.5, 0.25)$ (DGP), (e) $(q_{in}, q_{on}) = (0.5, 0.4)$ (GP), (f) $(q_{in}, q_{on}) = (0.5, 0.4)$ (GP). In (a)–(e), the slow to start probability $p_b = 0.5$, while in (f) $p_b = 0.425$. The horizontal direction (from left to right) is space and the vertical direction (from down to up) is time.

distance between vehicles in the downstream jam front. When the average distance between vehicles is small enough, it is possible that the free driving effect is weaker than the anticipation effect. Thus, synchronized flow can be formed at the downstream of wide moving jams.

Finally, the impact of the safe space gap d_{safe} and the critical velocity v_c on the outflow of wide moving jams is investigated. Comparing Fig. 5(a) with (b), the following conclusions can be made: (i) Both them have nothing to do with the synchronized outflow. (ii) Without the critical velocity v_c, the free outflow could not be simulated. Actually, considering v_c helps to enhance free driving effect. Thus, it is possible that the free driving effect is stronger than the anticipation effect, which means free outflow can be reproduced.

5. Conclusion

The improved average space gap cellular automaton model (IASGM) within the fundamental diagram approach has been proposed by taking the velocity effect and critical velocity into

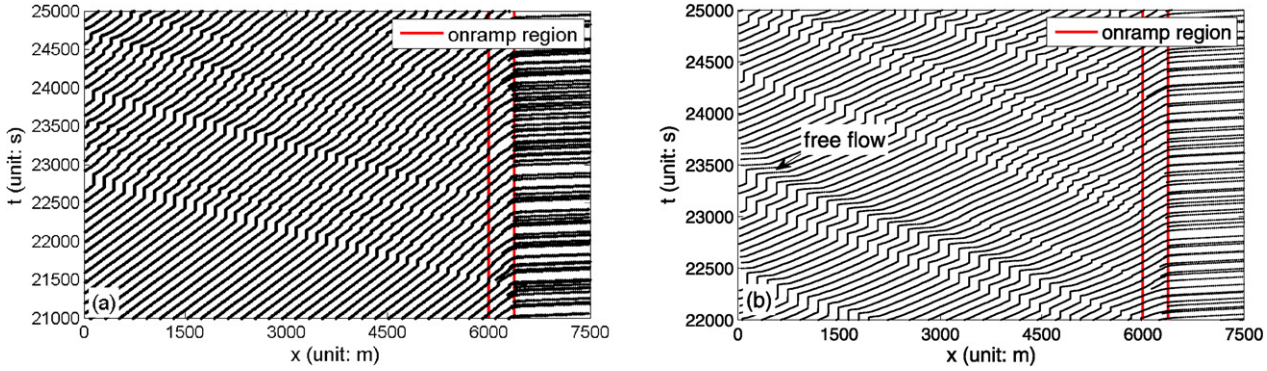

Fig. 5. Trajectories of every 20th vehicle. (a) $(q_{in}, q_{on}) = (0.8, 0.8)$, (b) $(q_{in}, q_{on}) = (0.4, 0.3)$. In (a) $v_c = 0$, $d_{safe} = 7$, while in (b) $v_c = 3$, $d_{safe} = v_{max}$. $L_{ramp} = 250$, $p_b = 0.425$ in (a), (b). The horizontal direction (from left to right) is space and the vertical direction (from down to up) is time.

account. The physics of traffic breakdown is explained by the competition between two opposite tendencies, i.e. the tendency towards to free flow due to the free driving effect and the tendency towards to synchronized flow owing to the anticipation driving effect. The probabilistic nature of traffic breakdown is simulated. The significant contribution is the discovery that the occurrence of synchronized outflow of wide moving jams has a close relationship with drivers time delay in acceleration at the downstream jam front, and the emergence of free outflow is closely connected with the critical velocity.

Except for above investigations of IASGM in this Letter, there are still many other features worth studying in the future. Firstly, the microscopic properties, such as the time headway distributions, the empirical optimal velocity functions. It has been reported that the time headway distribution has a cut off at the small time headway, which is less than one second [40,41]. Obviously, it is impossible for the ASGM due to the lack of velocity effect. Secondly, the two-lane version of IASGM should be developed. It will be very interesting to simulate and compare the results with [24]. [24] argues that macroscopic and microscopic spatiotemporal effects of the entire complexity of traffic congestion observed up to now in real measured traffic data can be explained by simulations of traffic flow consisting of identical drivers and vehicles, if a microscopic model used in these simulations incorporates the fundamental hypothesis of three-phase theory. Finally, whether the occurrence of synchronized outflow of wide moving jams depends on drivers time delay in acceleration at the downstream jam front or not should be surveyed in other traffic flow models.

Acknowledgements

We sincerely thank referees for their helpful suggestions. The manuscript has been improved according to the referees' comments. This work is partially supported by the Fundamental Research Funds for the Central Universities (2011YJS233, 2011YJS238), the National Natural Science Foundation of China (Grant Nos. 71071013, 71131001, 11001143), and 973 Program (No. 2012CB725403).

Appendix A

Three possibilities need to be analyzed separately to determine the value of v computed by $v = \min(d + \max(0, \min(v + 1, d, v_{max}) - d_{safe}), v_{max})$.

Case A. $\min(v+1, d, v_{max}) = v+1$ implying $d \geqslant v+1$ and $v_{max} \geqslant v+1$.

(1) Given that $v + 1 \geqslant d_{safe}$, leading to $v = \min(d + v + 1 - d_{safe}, v_{max})$, we have
- $d \leqslant v$ for $d + v + 1 - d_{safe} \leqslant v_{max}$, which exactly contradicts with $d \geqslant v + 1$, and
- $v = v_{max}$ for $d + v + 1 - d_{safe} > v_{max}$, which still contradicts with $v_{max} \geqslant v + 1$.

(2) Given that $v + 1 < d_{safe}$, leading to $v = \min(d, v_{max})$, we have
- $v = d$ for $d \leqslant v_{max}$, which exactly contradicts with $d \geqslant v + 1$, and
- $v = v_{max}$ for $d > v_{max}$, which still contradicts with $v_{max} \geqslant v + 1$.

Case B. $\min(v+1, d, v_{max}) = d$ implying $v + 1 \geqslant d$ and $v_{max} \geqslant d$.

(1) Given that $d \geqslant d_{safe}$, leading to $v = \min(2d - d_{safe}, v_{max})$, we have
- $v = 2d - d_{safe}$ and $d < d_c$ for $2d - d_{safe} \leqslant v_{max}$, where $d_c = \frac{d_{safe} + v_{max}}{2}$,
- $v = v_{max}$ and $d \geqslant d_c$ for $2d - d_{safe} > v_{max}$.

(2) Given that $d < d_{safe}$, leading to $v = d$.

Case C. $\min(v+1, d, v_{max}) = v_{max}$, implying $v + 1 \geqslant v_{max}$ and $d \geqslant v_{max}$. Then, we have

(1) $v = v_{max}$ and $d \geqslant v_{max}$ for $d + v_{max} - d_{safe} \geqslant v_{max}$, and
(2) $d < d_{safe}$ for $d + v_{max} - d_{safe} < v_{max}$, which exactly contradicts with $d \geqslant v_{max}$.

Based on Cases B and C(1), we derive

$$v = \begin{cases} d: & \text{if } d < d_{safe} \\ 2d - d_{safe}: & \text{if } d_{safe} \leqslant d < d_c \\ v_{max}: & \text{if } d_c \leqslant d \end{cases} \tag{3}$$

Substituting $d = \frac{1}{K} - L_{car}$ into Eq. (3), where K is the density, the velocity–density relationship is acquired:

$$v = \begin{cases} v_{max}: & \text{if } K \leqslant K_c \\ \frac{2}{K} - L_{car} - \frac{1}{K_{safe}}: & \text{if } K_c < K \leqslant K_{safe} \\ \frac{1}{K} - L_{car}: & \text{if } K_{safe} < K \leqslant K_{max} \end{cases} \tag{4}$$

Here, $K_{max} = \frac{1}{L_{car}}$, $K_c = \frac{2}{d_{safe} + v_{max} + 2L_{car}}$ and $K_{safe} = \frac{1}{d_{safe} + L_{car}}$. Let J denote the flux, accordingly, the flux-density relationship (i.e. the fundamental diagram) is derived:

$$J = \begin{cases} K v_{max}: & \text{if } K \leqslant K_c \\ 2 - K L_{car} - \frac{K}{K_{safe}}: & \text{if } K_c < K \leqslant K_{safe} \\ 1 - K L_{car}: & \text{if } K_{safe} < K \leqslant K_{max} \end{cases} \tag{5}$$

References

[1] F.A. Haight, Mathematical Theories of Traffic Flow, Academic Press, New York, 1963.
[2] G.B. Whitham, Linear and Nonlinear Waves, Wiley, New York, 1974.
[3] W. Leutzbach, Introduction to the Theory of Traffic Flow, Springer, Berlin, 1988.
[4] A. Schadschneider, Traffic and Granular Flow 97, Springer, Singapore, 1998.
[5] D. Chowdhury, L. Santen, A. Schadschneider, Phys. Rep. 329 (2000) 199.
[6] D. Helbing, Rev. Mod. Phys. 73 (2001) 1067.
[7] T. Nagatani, Rep. Prog. Phys. 65 (2002) 1331.
[8] B. Jia, Z.Y. Gao, K.P. Li, X.G. Li, Models and Simulations of Traffic System Based on the Theory of Cellular Automaton, Science, Beijing, 2007.
[9] B.S. Kerner, The Physics of Traffic, Springer, Berlin, 2004.
[10] B.S. Kerner, Introduction to Modern Traffic Flow Theory and Control, Springer, Berlin, 2009.
[11] M.J. Lighthill, G.B. Whitham, Proc. Roy. Soc. A 229 (1955) 281.
[12] P.I. Richards, Oper. Res. 4 (1956) 42.
[13] H.J. Payne, Trans. Res. Rec. 772 (1979) 68.
[14] H.J. Payne, in: Mathematical Models of Public Systems, Simulation Council Proceedings, 1971, pp. 51–61.
[15] G.F. Newell, Oper. Res. 9 (1961) 209.
[16] P.G. Gipps, Trans. Res. B 15 (1981) 105.
[17] K. Nagel, M. Schreckenberg, J. Phys. I 2 (1992) 2221.
[18] M. Bando, K. Hasebe, A. Nakayama, A. Shibata, Y. Sugiyama, Phys. Rev. E 51 (1995) 1035.
[19] D. Helbing, M. Treiber, Phys. Rev. Lett. 81 (1998) 3042.
[20] M. Treiber, A. Hennecke, D. Helbing, Phys. Rev. E 62 (2000) 1805.
[21] B.S. Kerner, H. Rehborn, Phys. Rev. E 53 (1996) R1297.
[22] B.S. Kerner, H. Rehborn, Phys. Rev. E 53 (1996) R4275.
[23] B.S. Kerner, H. Rehborn, Phys. Rev. Lett. 79 (1997) 4030.
[24] B.S. Kerner, Phys. Rev. E 85 (2012) 036110.
[25] B.S. Kerner, Phys. Rev. Lett. 81 (1998) 3797.
[26] B.S. Kerner, S.L. Klenov, J. Phys. A: Math. Gen. 35 (2002) L31.
[27] B.S. Kerner, S.L. Klenov, J. Phys. A: Math. Gen. 39 (2006) 1775.
[28] B.S. Kerner, S.L. Klenov, D.E. Wolf, J. Phys. A: Math. Gen. 35 (2002) 9971.
[29] B.S. Kerner, S.L. Klenov, M. Schreckenberg, Phys. Rev. E 84 (2011) 046110.
[30] H.K. Lee, R. Barlovic, M. Schreckenberg, et al., Phys. Rev. Lett. 92 (2004) 238702.
[31] W. Knospe, L. Santen, A. Schadschneider, et al., J. Phys. A 33 (2000) L477.
[32] R. Jiang, Q.S. Wu, J. Phys. A: Math. Gen. 36 (2003) 381.
[33] J.F. Tian, B. Jia, X.G. Li, R. Jiang, X.M. Zhao, Z.Y. Gao, Phys. A 388 (2009) 4827.
[34] K. Gao, R. Jiang, S.X. Hu, B.H. Wang, Q.S. Wu, Phys. Rev. E 76 (2007) 026105.
[35] B. Jia, X.G. Li, T. Chen, R. Jiang, Z.Y. Gao, Transpormetrica 7 (2011) 127.
[36] J.F. Tian, Z.Z. Yuan, M. Treiber, B. Jia, W.Y. Zhang, Phys. A 391 (2012) 3129.
[37] B.N. Persaud, S. Yagar, R. Brownlee, Trans. Res. Rec. 1634 (1998) 64.
[38] M.R. Lorenz, L. Elefteriadou, Trans. Res. Rec. 1776 (2001) 43.
[39] L. Elefteriadou, R.P. Roess, W.R. McShane, Trans. Res. Rec. 1484 (1995) 80.
[40] L. Neubert, L. Santen, A. Schadschneider, M. Schreckenberg, Phys. Rev. E 60 (1999) 6480.
[41] W. Knospe, L. Santen, A. Schadschneider, M. Schreckenberg, Phys. Rev. E 70 (2004) 016115.